



Title	Solid State Synthesis of Mg <sub>2</sub> Si/MgO Composites from an Elemental Mixture Powder of Magnesium and Rice Husk Silica
Author(s)	Umeda, Junko; Kondoh, Katsuyoshi; Kawakami, Masashi et al.
Citation	Transactions of JWRI. 2008, 37(1), p. 113-117
Version Type	VoR
URL	<a href="https://doi.org/10.18910/4713">https://doi.org/10.18910/4713</a>
rights	
Note	

*The University of Osaka Institutional Knowledge Archive : OUKA*

<https://ir.library.osaka-u.ac.jp/>

The University of Osaka

# Solid State Synthesis of Mg<sub>2</sub>Si/MgO Composites from an Elemental Mixture Powder of Magnesium and Rice Husk Silica<sup>†</sup>

UMEDA Junko\*, KONDOH Katsuyoshi\*\*, KAWAKAMI Masashi\*\*\* and IMAI Hisashi\*

## Abstract

*The utilization of silica particles originating in rice husks as reinforcements for magnesium is discussed. The reactivity of magnesium with silica particles in the solid state to synthesize magnesium silicide (Mg<sub>2</sub>Si) was investigated by DTA and XRD analysis. Finer silica particles were more effective for reacting with magnesium at low temperature due to the increase of their surface area in contact with magnesium. Amorphous silica was more useful for the reaction than the crystalline form. The reactivity of rice husk silica was superior to that of the conventional mineral silica particles because of not only its amorphous structure but the larger specific surface area caused by the pore structures. In the case of a green compact of the elemental mixture of silica particles and Mg powder, the silica particle size was not effective on the reactivity because the coarse particles are fractured into fine ones by cold compaction at the applied pressure of 600 MPa. The distribution of Mg<sub>2</sub>Si intermetallics in magnesium powder composites consolidated by the SPS process was investigated by XRD and SEM-EDS analysis. When the sintering temperature was over the exothermic temperature of the elemental mixtures of silica particles and Mg powder in the DTA profile, the synthesis of Mg<sub>2</sub>Si occurs completely during sintering. The density and hardness of their composites sintered over the ignition temperature of the DTA profile were remarkably high because of the good densification by the high reactivity and the distribution of Mg<sub>2</sub>Si hard compounds.*

**KEY WORDS:** (Rice Husk Silica) (Magnesium) (Mg<sub>2</sub>Si Solid State Reaction) (Amorphous)

## 1. Introduction

Rice husk is a useful biomass to produce both the biomass energy and high-purity SiO<sub>2</sub> particles, because it includes organics of about 70% or more and 15~20% amorphous silica<sup>1-2)</sup>. The latter is available to be used as raw materials such as the concrete reinforcements, ceramic materials, fertilizers, additives for foods and cosmetic products<sup>3-5)</sup>. Magnesium silicide (Mg<sub>2</sub>Si) is a famous material used as semi-conductors and for the reinforcement of aluminum and magnesium alloys. The previous work indicated that silica glass waste particles were employed as raw materials to form Mg<sub>2</sub>Si reinforcements of the magnesium alloy via a solid state reaction with magnesium powders by deoxidization. The magnesium powder composites with Mg<sub>2</sub>Si dispersoids showed a good mechanical property and wear resistance<sup>6)</sup>. In this study, the reactivity of rice husk silica particles with magnesium in a solid state is discussed. The effects of their particle size and crystalline structures on the reactivity are investigated by comparing the conventional mineral silica by the thermal analysis. The distribution of

Mg<sub>2</sub>Si intermetallics of magnesium powder composites was also investigated when using various kinds of silica materials.

## 2. Experimental

### 2.1 Preparation of rice husk silica particles

To prepare high-purity silica particles originating in rice husks, the citric acid (C<sub>6</sub>H<sub>8</sub>O<sub>7</sub>) leaching process was applied to raw rice husks before burning in air. The concentration and temperature of the acid solution was 5% and 323K, respectively. The leaching was effective for removing the metallic impurities by a chelate reaction, and for accelerating a hydrolysis of the organics of cellulose and hemi-cellulose in rice husks<sup>7)</sup>. After the acid leaching of rice husks for 900s and the water-rinsing treatment of them, they were burned at 1073K for 1.8 ks in air for the thermal resolution of these organics. Amorphous silica materials with a purity of 99% or more were obtained. The conventional ball milling process under a dry condition was applied for their fragmentation. Their particle size was controlled by changing the milling time. In this study, three kinds of silica materials, having

<sup>†</sup> Received on July 11, 2008

\* Specially Appointed Researcher

\*\* Professor

\*\*\* Graduate Student

Transactions of JWRI is published by Joining and Welding Research Institute, Osaka University, Ibaraki, Osaka 567-0047, Japan

## Solid State Synthesis of $Mg_2Si/MgO$ Composites from an Elemental Mixture Powder

a mean particle size ( $d_0$ ) of  $3.9\mu m$ ,  $6.8\mu m$  and  $39.2\mu m$  measured by the particle distribution analyzer (HORIBA, Partica LA-920), were prepared. The annealing process at  $1423K$  for  $1.8\text{ ks}$  was applied to the amorphous rice husk silica materials to obtain the crystalline silica<sup>7)</sup>. On the other hand, the commercialized mineral crystalline silica particles ( $d_0=17.5\mu m$ ) were used as comparison materials of the rice husk silica.

### 2.2 Magnesium composites with $Mg_2Si$ dispersoids and their evaluation

Another raw material was magnesium powder with  $d_0$  of  $144.9\mu m$ . Each silica particle was mixed with Mg powders by the rocking milling equipment (Seiwa Giken Co. RM-05). Silica content was 10 mass% of the mixture. In general,  $Mg_2Si$  intermetallics are synthesized with an exothermic heat via the solid-state reaction between  $SiO_2$  and Mg<sup>8)</sup>. Therefore, DTA (Differential Thermal Analysis, Shimadzu DTG-60) evaluation was used to investigate the reaction behavior of each silica particle with magnesium powder during heating in an argon gas atmosphere. In particular, an ignition temperature of the exothermic heat in the DTA curve corresponds to the starting temperature of the above reaction to synthesize  $Mg_2Si$  intermetallics. XRD (X-ray Diffraction, Shimadzu XRD-6100) analysis was also applied to detect  $Mg_2Si$  peaks of the powder mixtures after annealing at some suitable temperatures. The green compact of each mixture powder was prepared by cold compaction at the applied pressure of  $600\text{ MPa}$ . DTA and XRD evaluation was also applied to the green compacts. An SPS (Spark Plasma Sintering, Syntech Co. SPS-1030S) process was employed to consolidate each elemental mixture powder, and to synthesize  $Mg_2Si$  in the solid state during sintering. The sintering was carried out at  $673K$  and  $773K$  for  $1.8\text{ ks}$  in vacuum. The applied pressure was  $30\text{ MPa}$  in the SPS process. The relative density and Rockwell (F scale) hardness of the sintered Mg powder materials were measured. XRD and SEM-EDS (Scanning Electron Microscope with Energy Dispersive Spectrometry, Joel JSM-6500F) analysis was carried out on the sintered materials to evaluate the synthesis of  $Mg_2Si$  intermetallics and their distribution.

## 3. Results and Discussion

### 3.1 Reactivity dependence on characteristics of silica particles and consolidation conditions

ICP analysis indicates the content of each silica powder originating from rice husks is 99% or more, and  $K_2O$  content, which is one of the major metallic impurities of rice husks, is less than 0.1%. This means the citric acid leaching process is effective for preparing high-purity silica particles from the husks. **Figure 1** shows XRD patterns of silica particles: amorphous rice husk silica with  $3.8\mu m$  (a), crystalline rice husk silica with  $3.8\mu m$  after annealed of  $1423K$  for  $1.8\text{ ks}$  (b), and crystalline mineral silica powder with  $17.5\mu m$  (c). The burning temperature of  $1073K$  is suitable to keep the amorphous structure of rice husk silica as described in the

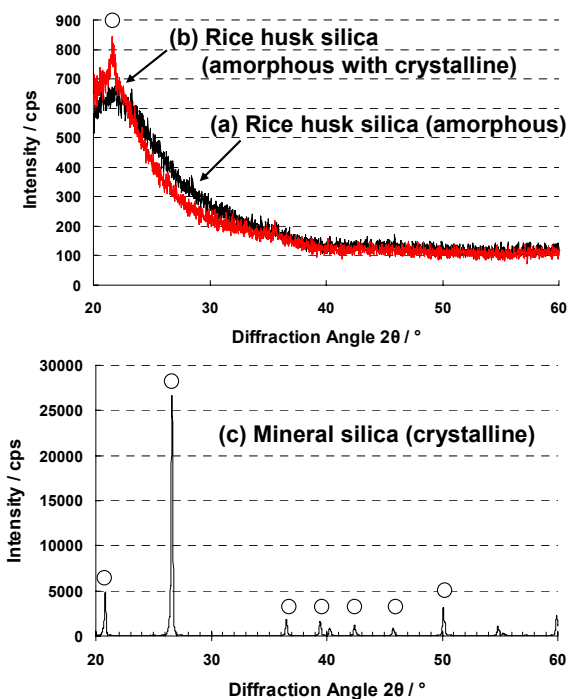


**Fig.1** XRD patterns of rice husk silica particles burned at  $1073K$  (a),  $1423K$  (b) and crystalline mineral silica particles (c).

previous work<sup>7)</sup>. On the other hand, the silica particles annealed at  $1423K$  clearly show a crystobalite peak with an amorphous structure as shown in (b). **Figure 2 (a)** reveals DTA curves of the elemental mixture of rice husk silica particles and Mg powders. All profiles show an exothermic heat due to the synthesis of  $Mg_2Si$  and an endothermic dip at the melt point of Mg ( $923K$ ). The exothermic behavior of each mixture powder is different. However, no remarkable difference of the endothermic behavior between the mixture powders is recognized. In the case of the silica materials with completely amorphous structures, **Fig.2 (b)** indicates that the ignition temperature gradually becomes higher with increase in the silica particle size. This is because the number of the contacted points of the silica particle surface with magnesium powders increases due to the increase of the specific surface area of silica particles when the particle size becomes small. The peak temperature also shows the same dependence on the silica particle size. With regard to the crystalline rice husk silica with  $3.9\mu m$ , it shows a high ignition temperature and a small exothermic heat, compared to the amorphous one with the same particle size. This result means that the crystalline silica particle has a poor reactivity with magnesium, and the solid-state reaction between the silica particles and magnesium powder did not effectively occur compared to the amorphous ones. **Figure 3** shows the DTA profiles of the green compacts of the elemental mixture of silica and magnesium powders. The difference of each ignition temperature is significantly small when using the amorphous silica materials with a different particle size. In the green compact, the contacted area of the fine silica

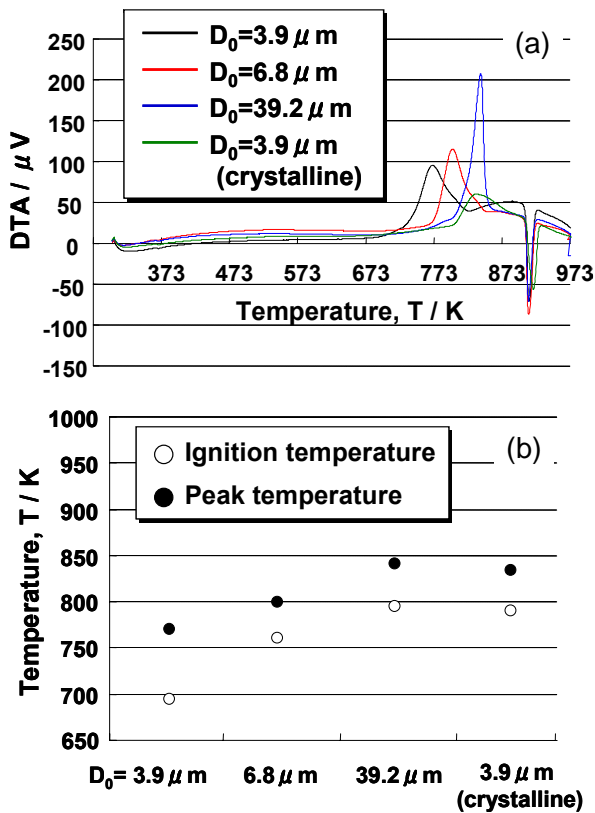


Fig.2 DTA profiles of elemental mixtures of silica particles and Mg powder (a), and dependence of ignition and peak temperature on silica particles size (b).

particle is almost same as that of the coarse one. It is easy to break the rice husk silica materials into fine particles by applying the compaction pressure of 600 MPa due to their porous structures. Therefore, the coarse rice husks silica particles are fractured into fine ones with  $1\text{--}5 \mu\text{m}$  by cold compaction, and their contacted surface area of the green compact drastically increases. Accordingly, the green compact consisting of amorphous silica materials with a different particle sizes, shows the same ignition and peak temperatures in the DTA profile. Compared to the crystalline rice husk silica and conventional mineral silica, the ignition temperature of the former is significantly low. This is due to the following two factors; (1) not only crystalline but amorphous structures

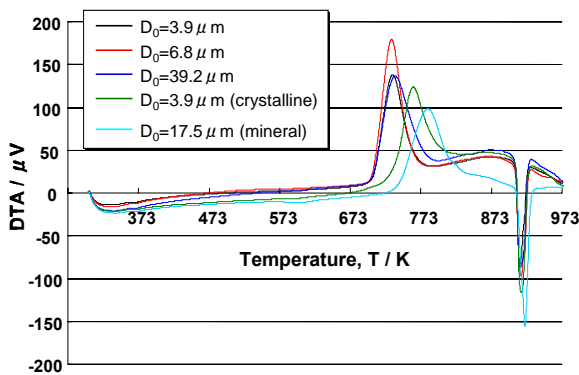


Fig.3 DTA profiles of green compacts of elemental mixtures of silica particles and Mg powder (silica content; 10mass%).

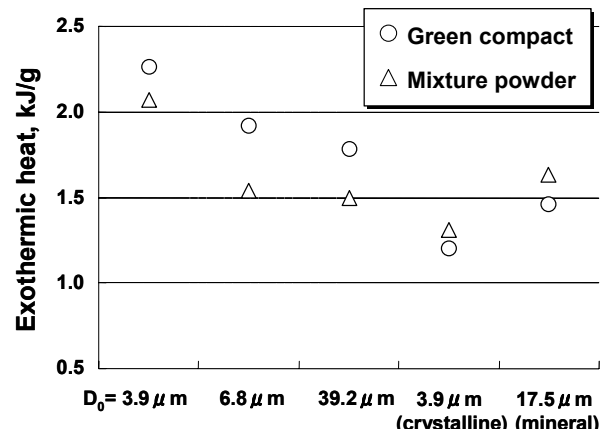


Fig.4 Dependence of exothermic heat in DTA profile of mixture powder and green compact on silica particle size.

are included in the former materials, (2) porous structures with a large surface area are effective for this reaction. Concerning the exothermic heat in the DTA profiles, as shown in Fig.4, the value of the green compact is larger than that of the mixture powder. This means the green compact has a superior reactivity between silica particles and Mg powder to the mixture powder, because its contacted area between them relatively increases by reducing the porosity at the primary particle boundaries in cold pressing. In both of the mixture powder and green compact, the exothermic heats gradually decreases with increase in the silica particle size. This means the reactivity of silica becomes poor, and the formation of  $\text{Mg}_2\text{Si}$  is controlled. In general, Mg atoms reacted with  $\text{SiO}_2$  at the silica particle surface, and the  $\text{Mg}_2\text{Si}$  layer is formed around the silica. When using the coarse silica particles, the Mg atoms diffusion takes a long time through the  $\text{Mg}_2\text{Si}$  layer into the core of silica<sup>9)</sup>. Therefore, the coarse silica materials have a poor reactivity with Mg powder to synthesize  $\text{Mg}_2\text{Si}$  in solid-state.

### 3.2 $\text{Mg}_2\text{Si}$ synthesis of Mg powder composites

The SPS process is applied to prepare the Mg powder composites with  $\text{Mg}_2\text{Si}$  intermetallics synthesized in the solid-state. The sintering temperatures are 673K and 773K. Amorphous silica with  $d_0=3.9 \mu\text{m}$  and mineral crystalline silica materials are used as raw powder. Figure 5 shows XRD patterns of each sintered material when using the elemental mixture powder of Mg-10%  $\text{SiO}_2$ . When applying the sintering temperature of 673K, both materials show a very small peak of  $\text{Mg}_2\text{Si}$ , and  $\text{MgO}$  peak is not also detected. Furthermore, the sintered material including the mineral silica has no change in  $\text{SiO}_2$  peak. These mean that no reaction between silica particles and Mg powder occurred during SPS at 673K. On the other hand, the sintered materials consolidated at 773K reveal  $\text{Mg}_2\text{Si}$  and  $\text{MgO}$  peaks resulting from the reaction between  $\text{SiO}_2$  particles and Mg powder. The above result corresponds well to the DTA profiles shown in Fig.2 and Fig.3. That is, the synthesis of  $\text{Mg}_2\text{Si}$  certainly takes place when the

## Solid State Synthesis of $Mg_2Si/MgO$ Composites from an Elemental Mixture Powder

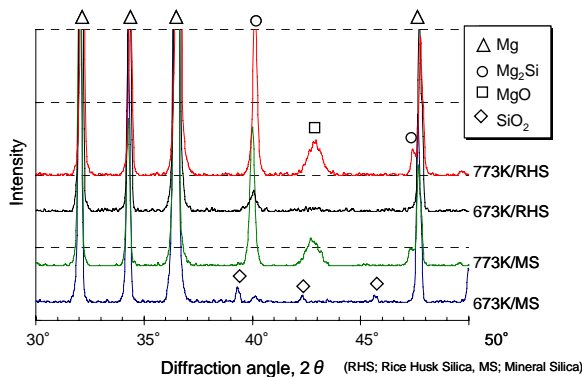


**Fig.5** XRD patterns of Mg powder material including various kinds of silica particles sintered by SPS at 673K and 773K.

sintering temperature is higher than the ignition temperature of its DTA profile. The relative density and Rockwell hardness of the sintered materials is shown in **Fig.6**. The density of both materials is over 99.5% when the sintering temperature of 773K is applied. The difference of HRF hardness between these sintered materials is small. In the case of the sintering at 673K, the sintered material including the rice husk silica particles shows a relative density of 99.3% and 29.8 HRF hardness. The decrease of density and hardness is due to the poor reactivity of rice husk silica particles with Mg powder at 673K compared to that in sintering at 773K. However, the sintered material including the mineral silica particles reveals a low density of 95.4%. It is impossible to measure HRF hardness of this material. That is, when using the mineral silica particles and sintering at 673K, the sinterability of Mg-10%  $SiO_2$  mixture powder is significantly reduced. It is considered that it is difficult to fracture the hard mineral silica particles compared to the rice husk ones with porous structures, and the densification is prohibited during consolidation by SPS process. Furthermore, no reaction between  $SiO_2$  and Mg powder at 673K caused to obstruct the sintering. **Figure 7** indicates SEM-EDS observation results on the sintered Mg powder material including the rice husk silica particles consolidated at 673K by the SPS process. Point (a) is bright at the primary Mg powder boundary, and corresponds to the additives of rice husk  $SiO_2$  particles. The mapping on point (b) around these silica particles reveals both Mg and Si, that is,  $Mg_2Si$  layers exist around the silica particles. As mentioned in Fig.5, this material contains a little  $Mg_2Si$  synthesized during SPS. The above results also mean the reaction between  $SiO_2$  and Mg powder does not completely occur after sintering at 673K due to the insufficient sintering temperature.

### 4. Conclusion

The reactivity of silica particles originated in rice husks with magnesium powder was examined. The effects of particle size and crystalline structure of the silica particles on the reactivity to synthesize  $Mg_2Si$  intermetallics in solid-state sintering were investigated by DTA and XRD analysis. Finer silica particles are more effective in

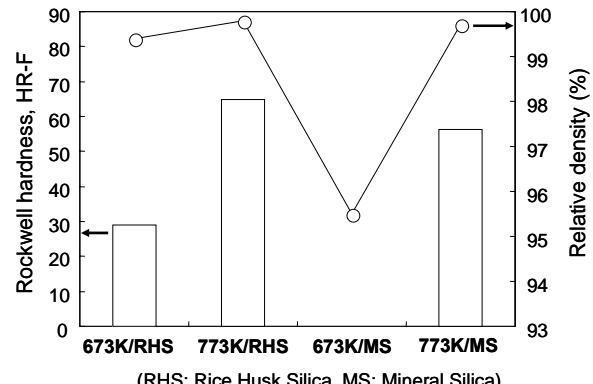


**Fig.6** Relative density and Rockwell hardness of Mg powder sintered material including various kinds of silica particles.

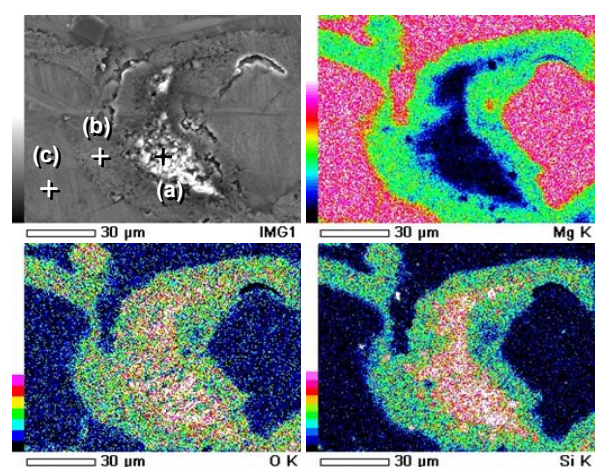


**Fig.7** SEM-EDS analysis of Mg powder material including rice husk silica sintered at 673K.

reacting with magnesium powders at low temperature due to the increase of their surface area contacted with the magnesium matrix powder. Amorphous silica is more useful for the reaction than crystalline one. The reactivity of rice husk silica is superior to that of the conventional mineral silica particles because of not only its amorphous structure but the larger specific surface area due to its pore structures. In the case of the green compact of the elemental mixture of silica particles and Mg powder, the silica particle size is not effective in the reactivity because the coarse particles are fractured into fine ones by cold compaction. When the sintering temperature is over the exothermic temperature of the mixture in the DTA profile, the synthesis of  $Mg_2Si$  completely occurs during sintering. On the other hand, the mineral silica particles are insufficient for the fabrication of Mg powder sintered materials with in-situ formed  $Mg_2Si$  compounds. This is because they lack the reactivity due to their crystalline structures, and are hard to be fractured during SPS process.

### Acknowledgement

This project is supported by “Research & Technology Development on Waste Management Research Grant”, Ministry of the Environment.

**References**

- 1) P. C. Kapur: Powder Tech.: 44 (1985), pp.63-67.
- 2) T. C. Luan and T.C Chou: Industrial & Engineering Chemistry Research, 29 (1990), pp.1922-1927.
- 3) M. Nehdi, J. D. Quette and A. E. Damatty: Cement and Concrete Research, 33 (2003), pp.1203-1210.
- 4) R. V. Krishnarao and M. M. Godkhindi: Ceramics International, 18 (1992), pp.185-191.
- 5) M. K. Naskar and M. Chatterjee: Journal of the European Ceramic Society, 24 (2004), pp.3499-3508.
- 6) H. Muramatsu, K. Kondoh, T. Aizawa: JSME International Journal, Series A, 46 (2003) pp.247-250.
- 7) J. Umeda, K. Kondoh, Y. Michiura: Materials Transactions, 48 (2007) pp.3095-3100.
- 8) K. Kondoh and T. Luangvaranunt: Materials Transactions, 44 (2003) pp.2468-2474.
- 9) K. Kondoh, H. Oginuma, A. Kimura, S. Matsukawa, and T. Aizawa: Materials Transactions, 44 (2003) pp.981-985.